Ultrasound in Med. & Biol., Vol. 44, No. 1, pp. 94–101, 2018

0301-5629/$ - see front matter

https://doi.org/10.1016/j.ultrasmedbio.2017.08.1884

● *Original Contribution*

HIGH-FREQUENCY ULTRASOUND IMAGING OF TIDEMARK *IN VITRO* IN ADVANCED KNEE OSTEOARTHRITIS

YAN-PING HUANG,*† JIN ZHONG,* JIE CHEN,*‡ CHUN-HOI YAN,§ YONG-PING ZHENG,* and CHUN-YI WEN*

* Interdisciplinary Division of Biomedical Engineering, Faculty of Engineering, The Hong Kong Polytechnic University, Hung Hom, Kowloon, Hong Kong SAR, China; † School of Electronic and Information Engineering, South China University of Technology, Guangzhou, China; ‡ Department of Orthopedics, Shanghai Institute of Traumatology and Orthopedics, Ruijin Hospital, Shanghai Jiaotong University School of Medicine, Shanghai, China; and § Department of Orthopaedics & Traumatology, Li Ka Shing Faculty of Medicine, The University of Hong Kong, Hong Kong, China

(*Received* 11 *April* 2017; *revised* 20 *July* 2017; *in final form* 28 *August* 2017)

Abstract—High-frequency ultrasound imaging has been widely adopted for assessment of the degenerative changes of articular cartilage in osteoarthritis (OA). Yet, there are few reports on investigating its capability to evaluate subchondral bone. Here, we employed high-frequency ultrasound imaging (25 MHz) to examine *in vitro* the tidemark in cylindrical osteochondral disks ($n = 33$) harvested from advanced OA knees of humans. We found good correspondence in morphology observed by ultrasound imaging and micro-computed tomography. Ultrasound roughness index (URI) of tidemark was derived from the raw radiofrequency signals to compare with bone quality factors, including bone volume fraction (BV/TV) and bone mineral density (BMD) measured by micro-computed tomography, using the Spearman correlation (ρ). URI of the tidemark was negatively associated with the subchondral plate BV/TV ($\rho = -0.73$, $p < 0.001$), BMD ($\rho = -0.40$, $p = 0.020$), as well as the underneath trabecular bone BV/TV ($\rho = -0.39$, $p = 0.025$) and BMD ($\rho = -0.43$, $p = 0.012$). In conclusion, this preliminary study demonstrated that morphology measured by high-frequency ultrasound imaging could reflect the quality of the subchondral bone. High-frequency ultrasound is a promising imaging tool to evaluate the changes of the subchondral bone in addition to those of the overlying cartilage in OA. (E-mail: chunyi.wen@polyu.edu.hk)

Key Words: **Osteoarthritis, Articular cartilage, Subchondral bone, High-frequency ultrasound, Tidemark, Roughness.**

INTRODUCTION

Osteoarthritis (OA) is a prevalent chronic musculoskeletal disease that affects millions of elderly people around the world. The hallmark of OA includes articular cartilage loss and subchondral bone disturbance (Li et al. 2013; Wen et al. 2014). Clinically, X-ray imaging is commonly used for the diagnosis of OA, with a typical joint space narrowing, osteophytosis, subchondral bone sclerosis and cystic lesion shown in radiography of an osteoarthritic joint (Altman et al. 1986). An X-ray–based assessment scheme, such as the Kellgren-Lawrence classification of knee OA, is widely used for grading the severity of this disease. However, it mainly reflects the pathologies of bone at an advanced stage and fails to detect the subtle changes of bone and cartilage at an early stage of the disease. Several magnetic resonance imaging (MRI) techniques have been well developed to assess the morphology of cartilage and bone in OA (Eckstein et al. 2006; Ristow et al. 2009), but the high cost of MRI examination and long scanning time for data acquisition limit its application for screening of knee OA. Arthroscopy is a minimally invasive approach to provide the information about the surface of articular cartilage directly, but it fails to probe the change in either the deep layer of cartilage or the subchondral bone (Chaturvedi et al. 2017).

Ultrasound assessment has been the subject of many scientific investigations related to OA. Clinical ultrasonography in the range of several MHz can be performed by placing probes on the skin and can detect some specific changes inside the joint such as synovitis; however,

Address correspondence to: Chun-Yi Wen, Department of Biomedical Engineering, Faculty of Engineering, The Hong Kong Polytechnic University, Hung Hom, Kowloon, Hong Kong SAR, China. E-mail: chunyi.wen@polyu.edu.hk

Table 1. Comparison between the present study and some previous work, using ultrasound for simultaneous cartilage and bone assessment

Study	Specimen, status	US freq (MHz)	US parameters				Reference method for bone
			Reflection—C	Reflection—CB	Roughness—C	Roughness—CB	
Brown et al. (2008)	Animal, OA	10	✓	✓	×	×	×
Saarakkala et al. (2006)	Animal, OA	20	✓	✓	✓	×	×
Niu et al. (2012)		55					
Aula et al. (2010)	Animal, Normal	5	✓	✓	✓	×	pQCT
Liukkonen et al. (2013)	Human, Normal	9	✓	✓	✓	×	μCT
This study	Human, OA	25	✓	✓	✓	✓	μCT

US = ultrasound; C = cartilage surface; CB = cartilage–bone interface (tidemark).

it is not sensitive enough to detect the early degeneration of articular cartilage when a relatively low frequency is used (Wang et al. 2010). Considering the limitations of conventional ultrasonography, high-frequency ultrasound (usually >20 MHz) uses a much higher resolution, allowing physicians to obtain a clearer view of the samples. Quite a number of studies have shown that ultrasonic signals coming from the articular cartilage surface bear the information related to osteoarthritic change. Ultrasonic parameters such as the surface reflection coefficient, backscattering coefficient and roughness index could reflect the quality of articular cartilage and enable us to distinguish between normal and degenerated articular cartilage at OA's early stage (Brown et al. 2008; Kiviranta et al. 2007; Männicke et al. 2014, 2016; Rohrbach et al. 2017; Saarakkala et al. 2004, 2006; Wang et al. 2010, 2014).

Anatomically, non-calcified articular cartilage is connected with subchondral bone through an osteochondral junction, which mainly consists of an intermediate calcified cartilage layer with two interfaces (*i.e.,* the tidemark on the cartilage side and the cement line on the bone side). The osteochondral junction is most vulnerable to macro- and micro-damages under mechanical stress, which will lead to tidemark disruption, angiogenesis and invasion of sensory nerves and blood vessels from the subchondral bone into the non-calcified cartilage at the onset of OA (Suri and Walsh 2012), and which may cause a significant change of morphology of this junction. Imaging of the osteochondral junction is desirable for early detection of OA.

Ultrasound has been proposed as a method to assess cartilage and bone simultaneously (Aula et al. 2010; Brown et al. 2008; Liukkonen et al. 2013; Niu et al. 2012; Saarakkala et al. 2006). The most commonly used parameters include the ultrasound reflection and surface roughness from the two interfaces (*i.e.,* the cartilage surface and the cartilage–bone interface). However, few studies have tried to evaluate the tidemark roughness using high-frequency ultrasound. In this study, we used high-frequency ultrasound for the purpose of assessing both the articular cartilage and the subchondral bone, using the parameters of ultrasound reflection and roughness measured at the two interfaces (*i.e.,* cartilage surface and tidemark). Table 1 provides a comparison of the differences of our study with some similar previous studies. In comparison with similar studies, we used parameters obtained from high-frequency ultrasound for the assessment of cartilage and subchondral bone quality in human osteoarthritic samples. Our hypothesis is the morphologic information measured at the tidemark, such as its roughness index, is closely related to the subchondral bone quality in an osteoarthritic joint.

MATERIALS AND METHODS

Sample preparation

Our institutional ethics committee approved all the experimental procedures (Ref No: UW-09368), and informed consent was obtained from each patient in this study. From February to April 2016 in one of the authors' institutes, osteochondral samples were collected from the tibial plateau of 10 patients (3 men, 7 women, age 72 ± 9 y) who received total knee replacement surgery because they had late-stage knee OA. First, 3~4 osteochondral disks with a diameter of 10 mm were drilled from each sample, with most harvested from the lateral side where more cartilage remained (Figs. 1a, 1b). A total of 33 osteochondral disks were collected from all the samples and frozen at −80°C before a series of experimental procedures, including ultrasound, micro-computed tomography (micro-CT) and histologic examinations in sequence.

Ultrasound imaging

Osteochondral disks were immersed in physiologic saline solution, thawed for a minimum 1 h, and then fixed with plastic clay (Blu-Tack, Bostik, Thomastown, Australia) at the bottom of a container for ultrasound measurement (Fig. 1c). Radiofrequency (RF) and B-mode

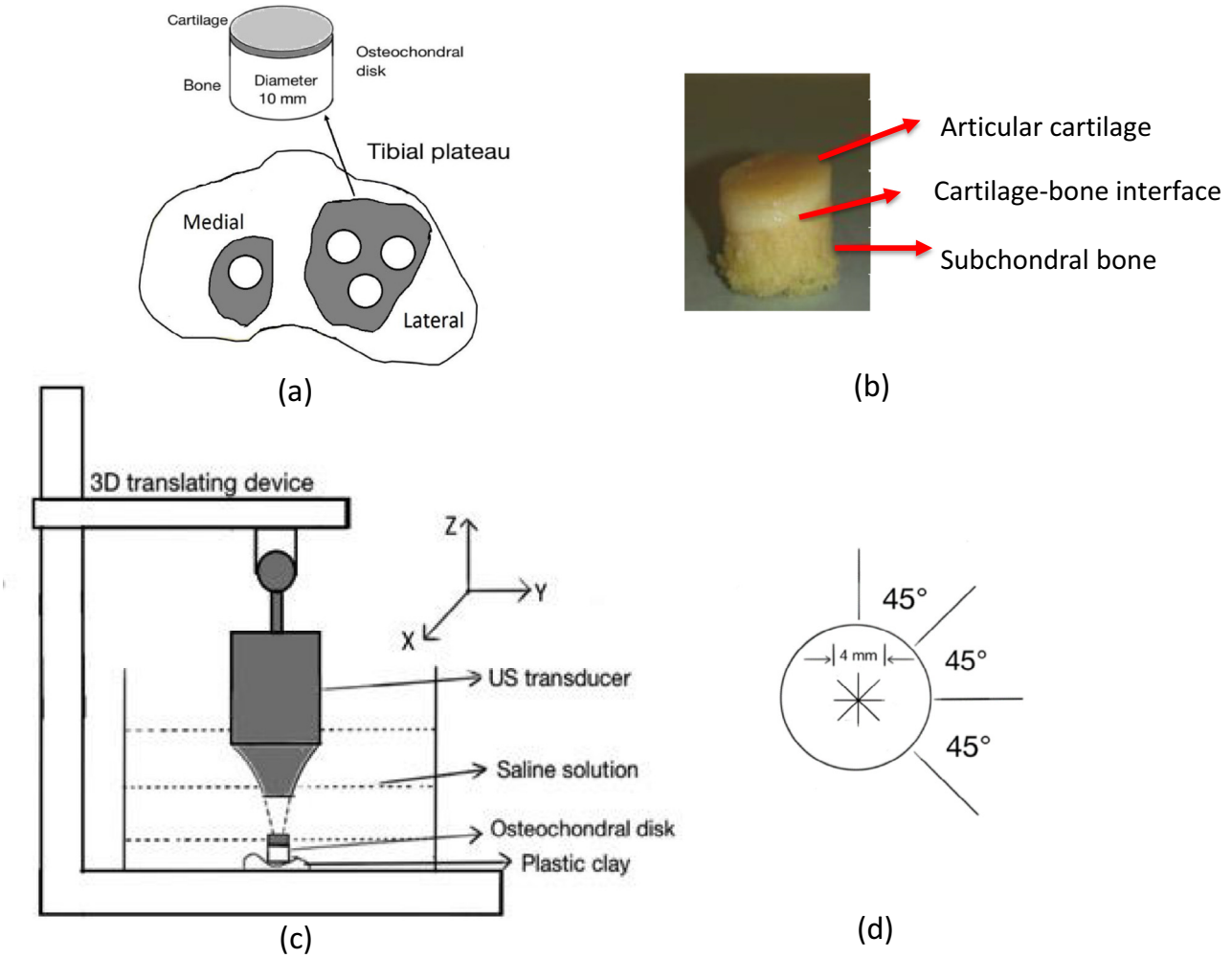

Fig. 1. (a) Osteochondral disks of 10 mm in diameter were extracted for this experimental test. (b) An osteochondral disk with articular cartilage (*top*) and subchondral bone (*bottom*). (c) How an osteochondral disk was positioned for ultrasound measurement. (d) The four scan directions for an osteochondral disk. Please refer to the text for details.

ultrasound signals were collected, using a linear array transducer (MS550 D, VisualSonics, Inc., Toronto, ON, Canada) of a high-frequency ultrasound imaging system (Vevo LAZR, VisualSonics, Inc.). Multiple focuses could be set for imaging, but, for the ease of RF signal processing, a single focus was set and was placed at the position of the tidemark (*i.e.,* the second bright line seen in the ultrasound image of the disk). The −3 dB bandwidth was 17–33 MHz with a central frequency of 25 MHz for the chosen transducer, which was experimentally determined by measuring the reflected pulse from a polished steel plate. Axial and lateral resolutions of the transducer were 40 μm and 80 μm, respectively, according to information from the manufacturer. The transducer could be translated in three directions and rotated when fixed in a positioning system (Fig. 1c), and it was adjusted to obtain a maximally reflected signal from the cartilage surface before data collection, indicating an optimized perpendicularity between the ultrasound beam and the cartilage surface. For spatial averaging, the sample container was horizontally rotated along the center of the disk and the scanning process was repeated in four directions with an angular interval of 45° in the horizontal plane (Fig. 1d). Average results from the four scans were used to represent the properties of that sample. Ultrasound signals were digitized as 32-bit floating data at an equivalent sampling rate of 1000 MHz and stored for off-line processing.

Extraction of ultrasound parameters for quantitative analyses

From the obtained ultrasound signals we calculated the following parameters: integrated reflection coefficient (IRC) and ultrasound roughness index (URI) of the cartilage surface, the tidemark and cartilage thickness. Details of the extraction of parameters can be found in our earlier reports (Wang et al. 2010, 2014), and related

Table 2. Ultrasound parameters measured from the osteochondral disk

Cartilage thickness	*IRC*	*URI*
$\frac{cT_{tof}}{2}$	$\frac{1}{\Delta f}\int_{f_1}^{f_2} R_c^{dB} df$	$\sqrt{\frac{1}{m}\sum_{i=1}^{m}(d_i-\bar{d})^2}$

c: speed of ultrasound in cartilage, T_{tof}: time of flight between the two interface echoes.
IRC: integrated reflection coefficient, $R_c^{dB}(f)$ is the corrected frequency-dependent reflection coefficient in unit of dB, Δf is the −3 dB bandwidth from $f_1 = 17$ MHz to $f_2 = 33$ MHz. A window of 0.4 µs in length was used to gate the signal at the two interfaces for spectral analysis; URI: ultrasound roughness index, $m = 148$ is the total number of points for the surface profile used in the present study, d_i is the surface position at point i and $\bar{d}$ is the smoothed surface profile after compensating the natural curvature of the cartilage surface.

calculation methods of thickness, IRC and URI are presented in Table 2. In brief, the thickness of articular cartilage was determined by multiplying the time of flight of the ultrasound inside the cartilage layer (Fig. 2a) by a constant speed of sound of articular cartilage (1620 m/s) (Myers et al. 1995). IRC reflects the strength of the ultrasound reflection at a tissue interface (Fig. 2a) because of the acoustic impedance difference on both sides. The reflection spectrum was first corrected by a calibration spectrum measured from a reference steel plate placed at the same distance and then spatially averaged, before finally being averaged within the −3 dB bandwidth to obtain IRC. A window of 0.4 µs (about 400 points) in length was used to gate the signal for spectral analysis. For the tidemark, the sample specific reflection at the cartilage surface and the attenuation caused by the overlying cartilage layer were also corrected (Saarakkala et al. 2006) using an average attenuation coefficient of 0.27 dB/MHz/mm (Nieminen et al. 2004). For URI, a surface profile was first obtained by detecting the surface point from the RF signal, subtracted by its natural curvature, and then a standard deviation was calculated to represent the surface roughness of the interface. A total number of 148 lines were obtained for the scan length of 4 mm so the interval between each 2 lines was 27 µm. Note that, with the current setup, the sensitivity of the URI measurement was degraded at the cartilage surface compared with the tidemark because the focus was placed at the tidemark. Typical images of an osteochondral disk and the detected interface profiles are shown in Figure 2b. To be different from that of the cartilage, ultrasound parameters with a subscript of *bone* were used to indicate measurement from the tidemark. All

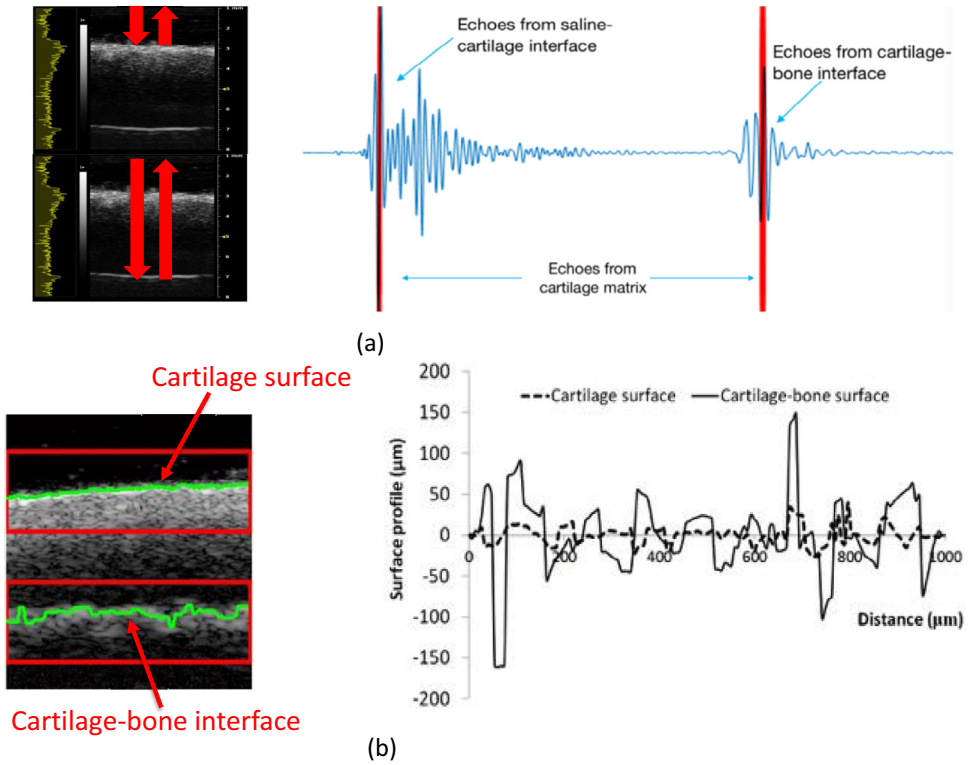

Fig. 2. (a) *Left*: interactions of ultrasound beam (*red*) with the two main interfaces, *i.e.,* the cartilage surface and the cartilage bone interface. *Right*: typical ultrasound signal of an osteochondral disk where the two echoes form the two interfaces. (b) *Left*: typical high-frequency ultrasound image showing where the two interfaces (*green*) are detected. *Right*: the surface profile signals obtained in ultrasound measurement where ultrasound roughness index (URI) can be further calculated.

ultrasound parameters were calculated using custom-written codes using Matlab (V.2014 b, Mathworks Inc., Natick, MA, USA) based on the RF signals collected from osteochondral disks.

Micro-CT examination

Micro-CT was performed to obtain a 3-D structure of the subchondral bone for assessing its bone quality and quantity after ultrasound measurement, using our established protocol (Wen et al. 2013). In brief, osteochondral disks were scanned by a micro-CT system (VivaCT 40, Scanco Medical AG, Bruttisellen, Switzerland) with an isotropic voxel size of $21 \times 21 \times 21$ μm^3. Bone 3-D structures were generated and quantitatively analyzed *via* the associated micro-CT software (Scanco Medical AG) for both the subchondral plate and subchondral trabecular bone. For the subchondral plate, bone mineral density (BMD), bone volume fraction (BV/TV) and cortical thickness (Ct.Th) were measured. For trabecular bone, bone parameters including BMD, BV/TV, trabecular thickness (Tb.Th), trabecular separation (Tb.Sp) and connection density (Conn.D) were measured.

Histologic examination

After micro-CT scanning, the samples were decalcified and embedded in wax sequentially for routine histopathologic examination, using our established protocol (Wen et al. 2013). The samples were positioned along the direction of ultrasound imaging and sectioned at 5 μm in thickness for hematoxylin and eosin staining.

Statistical analysis

Nonparametric Spearman correlation was used to analyze the relationship between ultrasound and micro-CT bone parameters and between ultrasound parameters of cartilage and tidemark. A confidence level of $p < 0.05$ was used to indicate a significant difference or correlation. All statistical analyses were performed with SPSS (v.21, IBM SPSS Inc., Chicago, IL, USA).

RESULTS

Ultrasound, micro-CT and histologic imaging of the cartilage–bone interface

As shown in Figure 3, the ultrasound images clearly delineate two interfaces in the human knee OA samples.

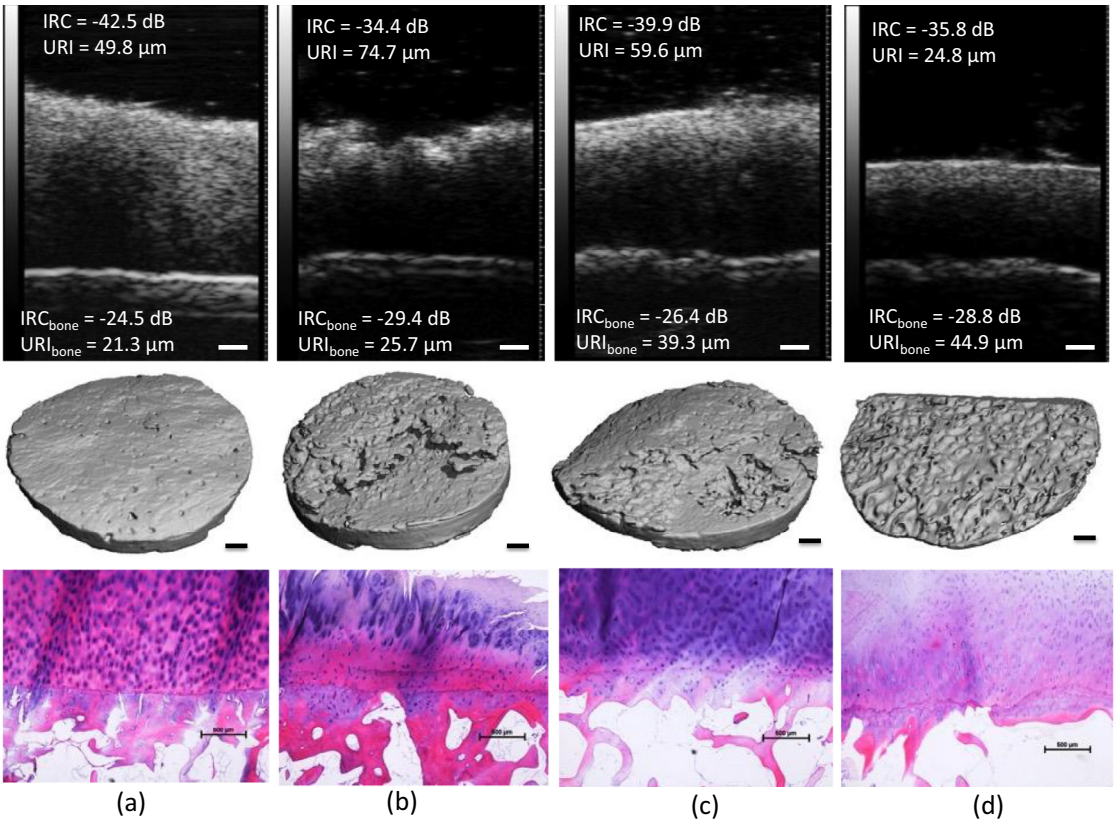

Fig. 3. Typical results for ultrasound imaging (*top row*), micro-CT (*middle row*) and histology (*bottom row*) among various osteochondral disks with various morphologies of the tidemark in human knee OA samples. (a) Smooth tidemark, (b) double tidemark and (c) and (d) intermediate levels of tidemark smoothness. Scale bars indicate a distance of 500 μm.

Table 3. Spearman correlation (ρ) between the measured ultrasound parameters and micro-CT parameters

	Micro-CT parameters of subchondral plate			Micro-CT parameters of subchondral trabecular bone					
Ultrasound parameters	BMD	BV/TV	Ct.Th	BMD	BV/TV	Tb.Sp	Tb.Th	Tb.N	Conn.D
IRC	–0.20	–0.10	–0.22	–0.15	–0.15	0.11	–0.02	–0.17	–0.23
URI	0.13	0.18	0.41*	0.38	0.34	–0.27	0.33	0.33	0.34
Cart.Th	0.01	–0.002	0.29	0.02	–0.02	–0.24	–0.11	0.29	0.28
IRC_{bone}	–0.12	0.07	0.17	0.24	0.25	–0.40*	0.10	0.44*	0.44*
URI_{bone}	–0.40*	–0.73‡	–0.45†	–0.43*	–0.39*	0.33	–0.52†	–0.30	–0.26

Cart.Th = cartilage thickness; BMD = bone mineral density; BV = bone volume; TV = tissue volume; Ct.Th = cortical thickness; Tb.Sp = trabecular space; Tb.Th = trabecular thickness; Tb.N = trabecular number; Conn.D = connection density.
Level of significance: * $p < 0.05$, † $p < 0.01$, ‡ $p < 0.001$.

One is the water–articular cartilage surface interface. The second is the cartilage–bone interface. High-frequency ultrasound images of the disintegrated cartilage–bone interface in knee OA samples were consistent with the rough surface of the subchondral bone plate in micro-CT images and also the irregular, discontinuous or double tidemark histopathologically (Fig. 3).

Quantitative parameters and correlation analyses

IRCs were –40.1 ± 3.6 dB at the articular cartilage surface and –24.0 ± 7.7 dB at the tidemark (*i.e.,* cartilage–bone interface) in all knee OA samples (n = 33). URI of the cartilage surface and the tidemark was 64.1 ± 25.8 μm, and 36.8 ± 7.4 μm, respectively. The thickness of the articular cartilage measured under high-frequency ultrasound was 2.66 ± 0.79 mm.

For the correlation analysis, the IRC significantly correlated with the URI of the cartilage interface ($\rho = –0.55$, $p < 0.001$) (Fig. 4a). The correlations between the ultrasound and micro-CT parameters are presented in Table 3. Most of the ultrasound parameters of the cartilage interface had no significant correlation with the micro-CT parameters of the subchondral bones, except a weak association between URI and cortical thickness ($\rho = 0.41$, $p = 0.017$).

IRC_{bone} was found to have no significant correlation with the subchondral plate ($p > 0.05$), but with some of the trabecular bone parameters, including trabecular separation (Tr.Sp) ($\rho = –0.40$, $p = 0.020$), trabecular number (Tr.N) ($\rho = 0.44$, $p = 0.011$) and Conn.D ($\rho = 0.44$, $p = 0.011$). URI_{bone} was significantly correlated with most of the bone parameters, including BMD ($\rho = –0.40$, $p = 0.020$), BV/TV ($\rho = –0.73$, $p < 0.001$) and Ct.Th ($\rho = –0.45$, $p = 0.008$), of the subchondral bone plate and BMD ($\rho = –0.43$, $p = 0.012$), BV/TV ($\rho = –0.39$, $p = 0.025$) and Tb.Th ($\rho = –0.52$, $p = 0.002$) of the subchondral trabecular bone. The strongest correlation between ultrasound and micro-CT parameters was found between URI_{bone} and BV/TV of the subchondral bone plate (Fig. 4b).

DISCUSSION

The present study adopted two parameters of the second interface (IRC_{bone} and URI_{bone}) derived from high-frequency ultrasound imaging of the osteochondral disks for nondestructive evaluation of microscopic change at the osteochondral junction. It is well known that the reflection of the ultrasonic wave from the osteochondral junction was mainly from the interface between calcified and noncalcified cartilage, that is, the tidemark (Modest et al. 1989). In this sense, both IRC_{bone} and URI_{bone} mainly reflected the changes of tidemark in OA.

Comparisons between previous and the current studies are summarized in Table 1. Ultrasound was proposed for the measurement of subchondral bone in previous studies. To penetrate deeper in the bone, an ultrasound frequency as low as 5 MHz was proposed for the measurement of the cartilage and bone simultaneously (Aula et al. 2010). In that study, the integrated backscattering of the bone, rather than IRC_{bone}, was found to have a significant correlation with the BMD of the subchondral plate. Possibly because of poor resolution, the URI of the tidemark was not specifically investigated in that study. In comparison with previous studies, this study adopted parameters obtained from high-frequency ultrasound for the assessment of cartilage and subchondral bone quality in human OA samples. We first provided evidence suggesting URI_{bone} as an indicator for subchondral bone quality and quantity.

Mounting evidence has shown correlations between subchondral bone structure and articular cartilage degradation in early OA using various imaging modalities, such as MRI (Bolbos et al. 2008). We also performed the correlation analyses under ultrasound. URI_{bone}—a morphologic parameter of the tidemark—was found to be closely correlated with the subchondral bone plate and underneath trabecular bone mass and microstructure; however, most of the correlation coefficients were weak ($\rho^2 < 0.2$). URI_{bone} in particular strongly correlated with the bone quantity (BV/TV) of the subchondral bone plate ($\rho^2 > 0.5$) in addition to weak correlation with the bone quality (BMD) ($\rho^2 < 0.2$). Multivariate regression analysis further proved that BV/

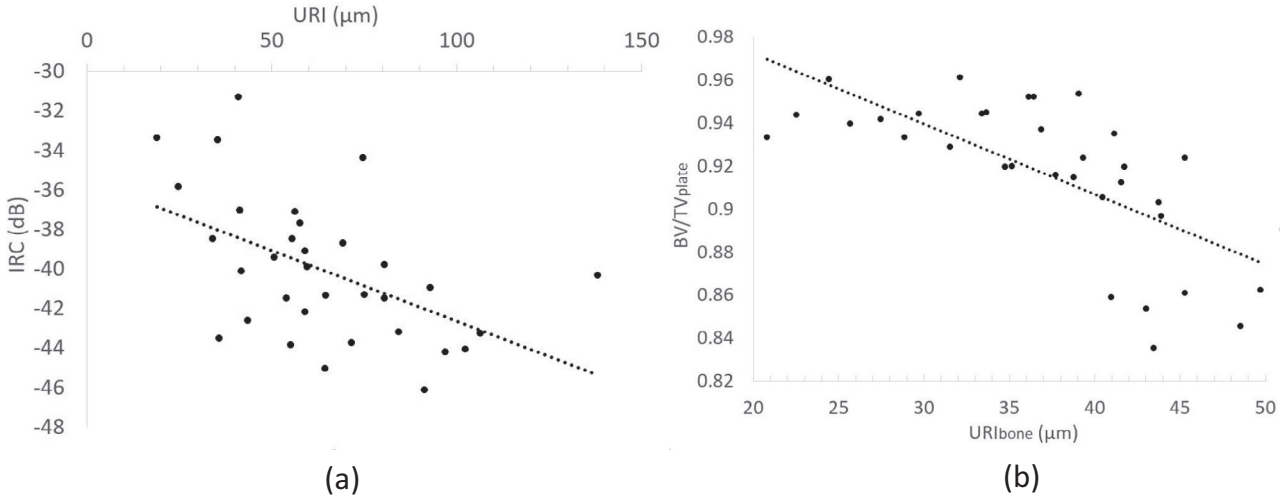

Fig. 4. (a) Spearman correlation ($\rho = -0.55$) between the cartilage surface roughness (URI) and the integrated reflection coefficient (IRC) from the cartilage surface and (b) Spearman correlation ($\rho = -0.73$) between ultrasound roughness index of the cartilage–bone interface (URI_{bone}) and the BV/TV of the subchondral bone plate (BV/TV_{plate}).

TV of the subchondral bone plate was a major independent variable to determine the roughness of tidemark as indicated by URI_{bone} (data not presented here). However, as shown in Figure 4, it was noted that URI_{bone} was negatively associated with subchondral plate BV/TV in a nonlinear manner. The decrease of subchondral plate BV/TV indicated a loss of structural integrity and an increase of subchondral plate porosity, which might allow new blood vessels and nerves growing and breaching the osteochondral junction in the early stage of OA (Suri and Walsh 2012). Our findings prompt the need for further investigation into the temporal changes of URI_{bone} in the process of OA development to test whether URI_{bone} could be a robust imaging biomarker for early OA.

Tidemark serves as an interface between the uncalcified cartilage and the subchondral bone. Therefore, the changes in tidemark in OA detected by URI_{bone} might reflect not only the disturbance of subchondral bone but also articular cartilage degradation, particularly that in the deep zone. It has been demonstrated recently that the hypertrophic changes and apoptosis of articular chondrocytes could also be measured on the basis of ultrasound measurement (Rohrbach et al. 2017). Further investigation is needed to investigate the weight of the bone and the cartilage changes that might contribute to the roughness change of tidemark under ultrasonic measurement (Männicke et al. 2014). More parameters might also be considered in future ultrasound measurement to study the various aspects of changes in OA related to various parts of the structure including cartilage, bone and junction.

Originally, we expected that IRC_{bone} might also change with subchondral bone because of the change of acoustic impedance contrast at both sides of the tidemark. However, we found a lack of biophysically meaningful and statistically significant correlations between IRC_{bone} and subchondral bone changes in knee OA samples; however, a few weak correlations were coincidentally found between IRC_{bone} and trabecular bone parameters (Tr.Sp, Tr.N and Conn.D). The propagation path of the ultrasonic wave through the surface and various layers of cartilage would affect the calculation of IRC_{bone}. The effect should be precisely corrected theoretically, but difficult to achieve practically. Taken together, URI_{bone} appeared to be a relatively more reliable imaging parameter for the assessment of tidemark in OA.

Some major limitations existed in the present study. First, a fixed attenuation coefficient was used for the correction in calculation of IRC_{bone}, which was not precise enough to obtain the true value of this parameter and might affect the practical utility of this parameter. Second, the sample number ($n = 33$) was still quite small and might not be large enough to generalize our study conclusions. Third, this study was limited to a cross-sectional observation and all of samples were from late-stage OA knees, which might be the partial reason for a relatively low correlation between measured ultrasound parameters of tidemark and bone micro-CT parameters. It prompts the need to deploy it in a longitudinal study to generalize our findings. Finally, the clinical value of the current imaging approach remains questionable at this stage although it could be employed *in vitro* successfully. High-frequency ultrasound, while having good resolution, cannot penetrate deep into soft tissue. It remains a major practical issue to be addressed as an *in-vivo* noninvasive measurement. Intra-articular high-frequency ultrasound measurement through an arthroscopic portal, using a miniaturized

transducer, could be an alternative way to identify the microscopic changes at the tidemark in people who have severe pain but show no obvious radiologic changes (Huang and Zheng 2009; Liukkonen et al. 2014; Virén et al. 2009). However, arthroscopy is still a minimally invasive procedure, which is inappropriate for screening of early OA (Kiviranta et al. 2007).

CONCLUSIONS

The feasibility of using high-frequency ultrasound imaging for quantitatively assessing osteochondral junctions in knee OA has been demonstrated *in vitro* in this study. The results indicated that high-frequency ultrasound can be a potential tool to measure the morphologic (particularly the roughness index) change of the osteochondral junction, particularly the tidemark, as reflection of change of the subchondral bone quality and quantity or deep cartilage degradation in OA. Further research is needed to demonstrate that this method can be used as a clinical tool to measure the change of articular cartilage and subchondral bone simultaneously in osteoarthritis *in vivo*.

Acknowledgments—Hong Kong Health and Medical Research Fund Research Fellowship Scheme (Ref No. #01150087) supported this study.

REFERENCES

Altman R, Asch E, Bloch D, Bole G, Borenstein D, Brandt K, Christy W, Cooke T, Greenwald R, Hochberg M. Development of criteria for the classification and reporting of osteoarthritis: Classification of osteoarthritis of the knee. Arthritis Rheum 1986;29:1039–1049.

Aula AS, Töyräs J, Tiitu V, Jurvelin JS. Simultaneous ultrasound measurement of articular cartilage and subchondral bone. Osteoarthritis Cartilage 2010;18:1570–1576.

Bolbos RI, Zuo J, Banerjee S, Link TM, Ma CB, Li XJ, Majumdar S. Relationship between trabecular bone structure and articular cartilage morphology and relaxation times in early OA of the knee joint using parallel MRI at 3 T. Osteoarthritis Cartilage 2008;16:1150–1159.

Brown CP, Hughes SW, Crawford RW, Oloyede A. Joint laminate degradation assessed by reflected ultrasound from the cartilage surface and osteochondral junction. Phys Med Biol 2008;53:4123–4135.

Chaturvedi V, Thabah MM, Ravindran V, Kiely PDW. Medical arthroscopy: A tool for diagnosis and research in rheumatology. Int J Rheum Dis 2017;20:145–153.

Eckstein F, Burstein D, Link TM. Quantitative MRI of cartilage and bone: Degenerative changes in osteoarthritis. NMR Biomed 2006;19:822–854.

Huang YP, Zheng YP. Intravascular ultrasound (IVUS): A potential arthroscopic tool for quantitative assessment of articular cartilage. Open Biomed Eng J 2009;3:13–20.

Kiviranta P, Töyräs J, Nieminen MT, Laasanen MS, Saarakkala S, Nieminen HJ, Nissi MJ, Jurvelin JS. Comparison of novel clinically applicable methodology for sensitive diagnostics of cartilage degeneration. Eur Cell Mater 2007;13:46–55.

Li G, Yin J, Gao J, Cheng TS, Pavlos NJ, Zhang C, Zheng MH. Subchondral bone in osteoarthritis: Insight into risk factors and microstructural changes. Arthritis Res Ther 2013;15:223.

Liukkonen J, Hirvasniemi J, Joukainen A, Penttilä P, Virén T, Saarakkala S, Kröger H, Jurvelin JS, Töyräs J. Arthroscopic ultrasound technique for simultaneous quantitative assessment of articular cartilage and subchondral bone: An *in vitro* and *in vivo* feasibility study. Ultrasound Med Biol 2013;39:1460–1468.

Liukkonen J, Lehenkari P, Hirvasniemi J, Joukainen A, Virén T, Saarakkala S, Nieminen MT, Jurvelin JS, Töyräs J. Ultrasound arthroscopy of human knee cartilage and subchondral bone *in vivo*. Ultrasound Med Biol 2014;40:2039–2047.

Männicke N, Schöne M, Liukkonen J, Fachet D, Inkinen S, Malo MK, Oelze ML, Töyräs J, Jurvelin JS, Raum K. Species-independent modeling of high-frequency ultrasound backscatter in hyaline cartilage. Ultrasound Med Biol 2016;42:1375–1384.

Männicke N, Schöne M, Oelze M, Raum K. Articular cartilage degeneration classification by means of high-frequency ultrasound. Osteoarthritis Cartilage 2014;22:1577–1582.

Modest VE, Murphy MC, Mann RW. Optical verification of a technique for *in-situ* ultrasonic measurement of articular-cartilage thickness. J Biomech 1989;22:171–176.

Myers SL, Dines K, Brandt DA, Brandt KD, Albrecht ME. Experimental assessment by high-frequency ultrasound of articular cartilage thickness and osteoarthritic changes. J Rheumatol 1995;22:109–116.

Nieminen HJ, Saarakkala S, Laasanen MS, Hirvonen J, Jurvelin JS, Töyräs J. Ultrasound attenuation in normal and spontaneously degenerated articular cartilage. Ultrasound Med Biol 2004;30:493–500.

Niu HJ, Wang Q, Wang YX, Li DY, Fan YB, Chen WF. Ultrasonic reflection coefficient and surface roughness index of OA articular cartilage: Relation to pathological assessment. BMC Musculoskelet Disord 2012;13:34.

Ristow O, Steinbach L, Sabo G, Krug R, Huber M, Rauscher I, Ma B, Link TM. Isotropic 3D fast spin-echo imaging versus standard 2D imaging at 3.0 T of the knee—image quality and diagnostic performance. Eur Radiol 2009;19:1263–1272.

Rohrbach D, Inkinen SI, Zatloukalová J, Kadow-Romacker A, Joukainen A, Malo MK, Mamou J, Töyräs J, Raum K. Regular chondrocyte spacing is a potential cause for coherent ultrasound backscatter in human articular cartilage. J Acoust Soc Am 2017;141:3105–3116.

Saarakkala S, Laasanen MS, Jurvelin JS, Töyräs J. Quantitative ultrasound imaging detects degenerative changes in articular cartilage surface and subchondral bone. Phys Med Biol 2006;51:5333–5346.

Saarakkala S, Töyräs J, Hirvonen J, Laasanen MS, Lappalainen R, Jurvelin JS. Ultrasonic quantitation of superficial degradation of articular cartilage. Ultrasound Med Biol 2004;30:783–792.

Suri S, Walsh DA. Osteochondral alterations in osteoarthritis. Bone 2012;51:204–211.

Virén T, Saarakkala S, Kaleva E, Nieminen HJ, Jurvelin JS, Töyräs J. Minimally invasive ultrasound method for intra-articular diagnostics of cartilage degeneration. Ultrasound Med Biol 2009;35:1546–1554.

Wang SZ, Huang YP, Saarakkala S, Zheng YP. Quantitative assessment of articular cartilage with morphologic, acoustic and mechanical properties obtained using high-frequency ultrasound. Ultrasound Med Biol 2010;36:512–527.

Wang Y, Huang YP, Liu A, Wan W, Zheng YP. An ultrasound biomicroscopic and water jet ultrasound indentation method for detecting the degenerative changes of articular cartilage in a rabbit model of progressive osteoarthritis. Ultrasound Med Biol 2014;40:1296–1306.

Wen C, Lu WW, Chiu KY. Importance of subchondral bone in the pathogenesis and management of osteoarthritis from bench to bed. J Orthop Translat 2014;2:16–25.

Wen CY, Chen Y, Tang HL, Yan CH, Lu WW, Chiu KY. Bone loss at subchondral plate in knee osteoarthritis patients with hypertension and type 2 diabetes mellitus. Osteoarthritis Cartilage 2013;21:1716–1723.